Contrasting Effects of Sulfur Dioxide on Cupric Oxide and Chloride during Thermochemical Formation of Chlorinated Aromatics

ARTICLE *in* ENVIRONMENTAL SCIENCE AND TECHNOLOGY · NOVEMBER 2014

Impact Factor: 5.33 · DOI: 10.1021/es503679c · Source: PubMed

4 AUTHORS, INCLUDING:

Takashi Fujimori

Kyoto University

45 PUBLICATIONS **169** CITATIONS

SEE PROFILE

Kenji Shiota

Kyoto University

14 PUBLICATIONS **63** CITATIONS

SEE PROFILE

Masaki Takaoka

Kyoto University

161 PUBLICATIONS **1,046** CITATIONS

SEE PROFILE

Environmental Science & Technology

Article

pubs.acs.org/est

Contrasting Effects of Sulfur Dioxide on Cupric Oxide and Chloride during Thermochemical Formation of Chlorinated Aromatics

Takashi Fujimori,*[†,‡] Yoshihiro Nishimoto,[‡] Kenji Shiota,[‡] and Masaki Takaoka[†,‡]

[†]Department of Global Ecology, Graduate School of Global Environmental Studies and [‡]Department of Environmental Engineering, Graduate School of Engineering, Kyoto University, Katsura, Nisikyo-ku, Kyoto 615-8540, Japan

Supporting Information

ABSTRACT: Sulfur dioxide (SO_2) gas has been reported to be an inhibitor of polychlorinated dibenzo-*p*-dioxins and furans (PCDD/Fs) formation in fly ash. However, other research has suggested little or no inhibitory effect of SO_2 gas. Although these studies focused on reactions between SO_2 gas and gas-phase chlorine (Cl) species, no attention was paid to thermochemical gas−solid reactions. In this study, we found contrasting effects of SO_2 gas depending on the chemical form of copper (CuO vs $CuCl_2$) with a solid-phase inorganic Cl source (KCl). Chlorinated aromatics (PCDD/Fs, polychlorinated biphenyls, and chlorobenzenes) increased and decreased in model fly ash containing CuO + KCl and $CuCl_2$ + KCl, respectively, with increased SO_2 injection. According to in situ Cu K-edge and S K-edge X-ray absorption spectroscopy, Cl gas and $CuCl_2$ were generated and then promoted the formation of highly chlorinated aromatics after thermochemical reactions of SO_2 gas with the solid-phase CuO + KCl system. In contrast, the decrease in aromatic-Cls in a $CuCl_2$ + KCl system with SO_2 gas was caused mainly by the partial sulfation of the Cu. The chemical form of Cu (especially the oxide/chloride ratio) may be a critical factor in controlling the formation of chlorinated aromatics using SO_2 gas.

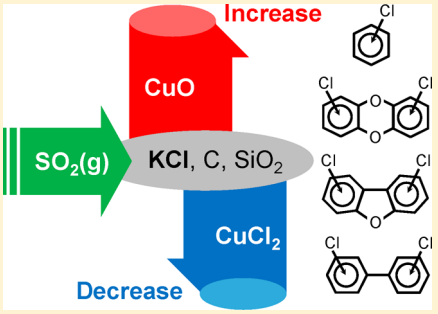

INTRODUCTION

Toxic chlorinated aromatic compounds (aromatic-Cls), such as polychlorinated dibenzo-*p*-dioxins (PCDDs), furans (PCDFs), biphenyls (PCBs), and benzenes (CBzs), become concentrated in fly ash during various anthropogenic incineration processes. Unburned carbon (C), chlorine (Cl), oxygen gas, and trace metal compounds are key in generating such aromatic-Cls.[1−5] To prevent the toxic and detrimental environmental effects of aromatic-Cls, thermal facilities should apply appropriate technologies to inhibit their formation.

A high-resolution quantitative study by Kimble and Gross reported minute traces (<1.2 ppt) of tetrachlorinated dibenzo-*p*-dioxin (TCDD) in fly ash collected from a coal-fired power plant, despite the presence of Cl and organic C in the system.[6] This finding indicated a specific inhibition mechanism of PCDD/Fs in coal fly ash. In particular, higher levels of sulfur (S) species, or the S/Cl ratio, in a coal-fired power plant were thought to be a key inhibitory feature from various experiments[7,8] on coal cofiring in municipal solid waste incinerators (MSWIs), a well-known thermal source of PCDD/Fs.[9]

Some inhibitory mechanisms related to S species have been proposed. Depletion of Cl_2 by sulfur dioxide (SO_2) through a gas-phase reaction was suggested by Griffin.[10] Thus,

$$Cl_2 + SO_2 + H_2O \rightarrow 2HCl + SO_3 \quad \text{(R1)}$$

A higher S/Cl ratio can decrease chlorination of the C matrix by a substitution reaction. Injection of SO_2 gas into the combustion process of liquid fuels in a pilot-scale plant showed an inhibitory effect on PCDD/F and chlorophenol (CP) formation.[11,12] SO_2 gas also inhibited toxic equivalent (TEQ) congeners of PCDD/Fs in MSWI fly ash collected from an electrostatic precipitator.[13] A reducing catalytic activity of copper (Cu) by S species was proposed by Gullett et al.[14] Thus,

$$CuO + SO_2 + \frac{1}{2}O_2 \rightarrow CuSO_4 \quad \text{(R2)}$$

CuO specifically catalyzes the Deacon reaction ($2HCl + {}^1/_2O_2 \rightarrow Cl_2 + H_2O$) and then promotes the formation of PCDDs.[15] Cupric sulfate ($CuSO_4$) is a less active catalyst of the Deacon reaction and biaryl synthesis of PCDDs via precursors such as CPs.[14] Based on these studies, SO_2 gas possibly plays an inhibitory role against PCDD/F formation in thermal processes.

In contrast, reports have described little or no inhibitory effect by S species. Mahle and Whiting showed that bituminous coal combustion produced PCDDs.[16] Coal cofiring in MSWI fly ash generated more PCDD/Fs than the firing of MSWI fly ash alone at a high S/Cl ratio.[17] Injection of SO_2 gas to a CuO(s), HCl(g), and phenol(g) system showed results comparable with no injection after heating at 300−500 °C in terms of total PCDD production.[14] Total PCDD/F concentrations were increased by SO_2 gas injection to MSWI fly ash under a Cl_2 stream at 400 °C[13] and a HCl/H_2O stream at 300

Received: July 29, 2014
Revised: October 23, 2014
Accepted: November 7, 2014
Published: November 7, 2014

°C.[18] These results suggest that S species (especially SO_2 gas) can also *promote* PCDD/F formation. However, to date, the role of SO_2 promoting activity has not been a major focus of research.

Previous studies have discussed reactions between gas-phase Cl species (Cl_2 or HCl) and SO_2 gas. MSWI fly ash generally contains percentage-order Cl combined with alkaline (earth) metals such as potassium (K), sodium, and calcium.[19,20] Although the main Cl species [i.e., potassium chloride (KCl), sodium chloride (NaCl), and $CaCl_2$] in the solid phase have small promoting effects in generating PCDD/Fs,[20,21] PCBs,[20,22] and CBzs[20,22] in MSWI fly ash, dramatic increases in such aromatic-Cls were found by adding trace amounts of cupric oxide (CuO)[22,23] and chloride ($CuCl_2$).[20,22,23] In fact, Cu in "real" MSWI fly ash exists mainly in chloride and oxide forms.[22,24,25] Such cupric compounds exhibit catalyst-like behaviors using solid-phase Cl species as a Cl sink. Thus, interactions among solid-phase Cl species, cupric compounds, and SO_2 gas remain unstudied in terms of their role and involvement in the mechanism with SO_2 gas in the thermochemical formation of aromatic-Cls.

In this study, we examined the influence of SO_2 gas on aromatic-Cl formation using model MSWI fly ashes (MFAs) containing a C source, base material, and a representative Cl source (KCl) with CuO and $CuCl_2{\cdot}2H_2O$. We quantified PCDD/Fs, PCBs, and CBzs through heating experiments, simulating the postcombustion zone, changing the concentrations of SO_2 gas (0, 500, 1000 ppm) with O_2 (10%; N_2 balance). Additionally, in situ observations of the Cu chemical form during heating MFAs under $SO_2/O_2/N_2$ and O_2/N_2 gas streams were conducted by measuring the Cu K-edge X-ray absorption near-edge structure (XANES). To better understand the behavior of solid-phase S, we measured and analyzed near-edge X-ray absorption structure (NEXAFS) of the S K-edge. Combining these quantitative and qualitative results, we discuss the contrasting effects and mechanisms of SO_2 gas on CuO and $CuCl_2$ during the thermochemical formation of aromatic-Cls.

MATERIALS AND METHODS

Sample Preparation. We prepared an MFA that was a mixture of cupric compounds such as CuO and $CuCl_2{\cdot}2H_2O$, KCl as a solid-phase Cl source, activated C (AC), and base materials such as silicon dioxide (SiO_2) and boron nitride (BN) containing 0.2% Cu, 10% Cl, 3.0% AC, and base material. Any organic compounds in the AC were removed by heating at 500 °C for 60 min under a stream of 100% nitrogen gas (100 mL/min).[26] According to previous studies,[22,23] we selected SiO_2 as a representative base material to measure the amount of aromatic-Cls. BN was used in X-ray absorption spectroscopic experiments because we needed to make a disk shape to measure in situ Cu K-edge XANES[24,27] and to avoid interference by Si K-edge absorption in the case of S K-edge NEXAFS measurements.[28] Previously, we reported that no significant difference existed in the formed content of aromatic-Cls between the use of BN and SiO_2.[24] We purchased SiO_2 (special grade), CuO (98%, special grade), $CuCl_2{\cdot}2H_2O$ (99%, special grade), and KCl (99.5% special grade) from Nacalai Tesque (Kyoto, Japan) and BN (special grade) from Wako Pure Chemical Industries, Ltd. (Osaka, Japan), and AC [Shirasagi palm shell, 20−48 mesh (number of holes/inch)] from Takeda Pharmaceutical Co., Ltd. (Osaka, Japan).

Measurement of Chlorinated Aromatic Compounds. The experimental heating procedure was as follows. We placed 5 g of MFA into a quartz boat contained within a quartz tube (120 × 4 cm internal diameter), which was then placed in a preheated electronic furnace at 300 °C for 30 min under a flow of 10% oxygen/90% nitrogen (O_2/N_2) delivered at 50 mL/min to simulate the postcombustion zone of an MSWI.[29] In this system, we controlled the SO_2 gas (0, 500, and 1000 ppm) as one of the gas stream components. After heating, the concentrations of aromatic-Cls in the MFA residue and in the gas phase collected in an impinger containing 100 mL of toluene were analyzed separately. The concentrations of PCDDs and PCDFs in MFAs were analyzed by high-resolution gas chromatography/high-resolution mass spectrometry (HRGC/HRMS).[25] In this study, PCBs and CBzs were analyzed by HRGC/low-resolution MS (GC-2010/GCMS-QP2010). Sample pretreatment for the determination of aromatic-Cls was according to Japanese Industrial Standards (JIS) K 0311 and 0312. For each heating experiment, analyses of the PCBs and CBzs were duplicated (n = 2). Previously, the concentrations of PCDDs and PCDFs in an MFA containing $CuCl_2{\cdot}2H_2O$ (MFA−$CuCl_2$) were measured three times (n = 3) to confirm reproducibility.[23] The concentrations of aromatic-Cls from the MFA−$CuCl_2$ showed small deviations of the same order as those from an MFA of a similar composition reported by Stieglitz et al.,[30] confirming the correctness of our analytical procedures. Subsequently, concentrations of PCDDs and PCDFs in MFAs were measured only once (n = 1). QA/QC was described in Supporting Information. Concentrations of PCDD/Fs, PCBs, and CBzs from MFAs containing CuO (MFA−CuO) and MFA−$CuCl_2$ are shown in Tables S1 and S2 (Supporting Information), respectively.

In Situ Cu K-edge XANES. Using in situ Cu K-edge XAFS, we detected the chemical structure of Cu at the atomic level in the MFA. After the MFA was ground using a pestle and agate mortar for 10 min, an appropriate amount of MFA was pressed into a disk. Cu K-edge XAFS was performed using beamline BL01B1 at SPring-8 (Hyogo, Japan). The MFA disk was heated in a T-type in situ cell consisting of a glass cell, a mantle heater, and a temperature controller (Figure S1A, Supporting Information).[24,27] The cell consisted of a tubular part (4.0 cm in diameter), and the "T" measured 11.5 cm on each side. The MFA disk was placed on a glass stand on a sample board and inserted into the cell. The X-rays passed through a window made of Kapton film. A water-cooled tube was coiled outside the Kapton film so that the thermal load did not affect the Kapton film. The temperature of the sample was increased gradually from room temperature to 400−450 °C (Figure S1B, Supporting Information). Temperature increase rates were 5 °C/min from room temperature to 100 °C and then 1 °C/min above 100 °C. The 10% O_2 (N_2 balance) or 1000 ppm of SO_2, 10% O_2 (N_2 balance) gaseous atmospheres were introduced from the inlet of the T-type cell at 50 mL/min and exhausted from the outlet. The Cu K-edge X-ray absorption fine structure could be measured in 120 s in "quick scan" mode with a Si(111) monochromator. After each measurement of a spectrum, a 180-s interval was needed to return the monochromator to the original position. XANES spectra of an MFA disk were collected with 19 solid-state detectors in fluorescence mode. The energies were first adjusted using the reference Cu foil. The spectra of reference materials, $CuCl_2{\cdot}2H_2O$, $CuCl_2$, CuCl, $Cu_2(OH)_3Cl$, CuO, Cu_2O, $CuSO_4$, copper sulfide (CuS), and Cu, were measured to compare their spectral shapes and to identify major species because an XANES

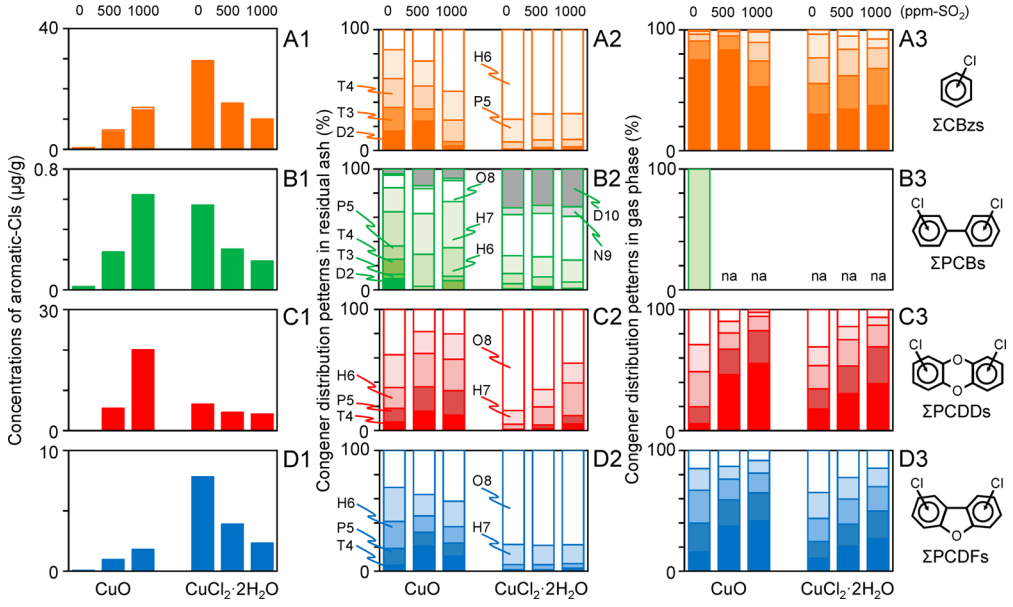

Figure 1. Concentrations and distribution patterns of CBzs, PCBs, PCDDs, and PCDFs in model fly ashes containing cupric oxide (CuO) and chloride ($CuCl_2 \cdot 2H_2O$) after heating at 300 °C for 30 min under an SO_2 gas stream (0, 500, and 1000 ppm). (A1–D1) Bar graphs: colored and white bars indicate the total concentrations in the residual ash and gas phase, respectively. (A2–D2) Congener distribution patterns in residual ash. (A3–D3) Congener distribution patterns in gas phase; na, not analyzed.

spectrum can be used as a fingerprint that reflects the local environment of the Cu. Species can be distinguished using the linear combination fit (LCF) technique, in which spectra of known reference species are fitted to the spectrum of the unknown sample. We used LCF to determine the major species using the REX 2000 software (ver. 2.5.5; Rigaku, Tokyo, Japan). The residual value,

$$R = \sum(\mathrm{XANES}_{\mathrm{measd}} - \mathrm{XANES}_{\mathrm{calcd}})^2 / \sum(\mathrm{XANES}_{\mathrm{measd}})^2$$

was used to evaluate the linear combination fit for the experimental spectra.

S K-edge NEXAFS. The S forms present after the MFA was heated were determined by measuring the S K-edge NEXAFS. An MFA was ground using a mortar for 10 min. The MFA powder was heated at 300 °C for 30 min under a flow of 1000 ppm of SO_2/10% O_2 (N_2 balance) delivered at 50 mL/min. After the heating procedure, MFA powder was sealed as quickly as possible and used for the measurement of S K-edge NEXAFS, performed using BL-11B at the Photon Factory (Tsukuba, Japan). An in situ cell could not be used at the Photon Factory because of physical restrictions on the device. Powdered MFA samples were mounted on carbon tape, and their XANES spectra were collected in total fluorescence yield (TFY) mode in a vacuum. Using normal AC, impure S in the AC influenced the result of S K-edge NEXAFS. So, we purchased high-purity AC (5N, 99.999%) from Sigma-Aldrich KK (Tokyo, Japan). The reference S compounds were $CuSO_4 \cdot 5H_2O$, CuS, K_2SO_4, and K_2S, and their XANES spectra were measured in total electron yield (TEY) mode in a vacuum. All S K-edge NEXAFS spectra were calibrated against the intense absorption feature of K_2SO_4 at 2480 eV. Based on these spectral features, analyses were performed between 2465 and 2495 eV by a linear combination fit using reference materials of S using the REX 2000 software.

RESULTS AND DISCUSSION

Concentrations of Aromatic-Cls. In the case with no SO_2 gas (i.e., O_2/N_2 gas only) stream, total concentrations of ∑CBzs, ∑PCBs, ∑PCDDs, and ∑PCDFs in MFA–CuO were 520, 20, 18, and 47 ng/g, respectively (Table S1, Supporting Information), and those in MFA–$CuCl_2$ were 29 000, 560, 6500, and 7800 ng/g, respectively (Table S2, Supporting Information). (∑ indicates the summation of all homologues of chlorinated aromatic compounds.) Amounts of aromatic-Cls in MFA–CuO and –$CuCl_2$ were consistent with our previous results using almost the same MFAs under an O_2/N_2 gas stream.[22,23] Thus, we confirmed the quantitative measurements of aromatic-Cls. Total WHO–TEQ concentrations of dioxin-like PCBs (DL-PCBs), PCDDs, and PCDFs in MFA–CuO had 0.047, 0.26, and 0.46 ng-TEQ/g, respectively (Table S1, Supporting Information), and those in MFA–$CuCl_2$ had 0.26, 7.7, and 21 ng-TEQ/g, respectively (Table S2, Supporting Information). Because MFA–CuO and –$CuCl_2$ showed higher concentrations of aromatic-Cls than MFAs without Cu compounds in previous studies,[22,23] the thermochemical behaviors of CuO and $CuCl_2$ apparently promoted aromatic-Cl formation.

SO_2 gas clearly influenced the thermochemical formation of aromatic-Cls (Figure 1). Most of the aromatic-Cls were generated in the residual ash, although trace aromatic-Cls were also detected in the gas phase through this heating experiment. Ash/gas ratios of aromatic-Cls showed the predominant proportion in the residual ash (Table S3, Supporting Information). With SO_2 gas flows, the ash/gas ratios of ∑CBzs, ∑PCDDs, and ∑PCDFs were ~10^1–10^2, 10^4, and 10^3–10^4, respectively (Figure S2, Supporting Information). Most gas-phase PCBs were below the detection limit of GC/MS. Thus, SO_2 gas mainly resulted in the solid-phase formation of aromatic-Cls.

The concentrations of aromatic-Cls suggested contrasting effects of SO_2 gas, depending on the Cu compounds in the model system. Aromatic-Cls generated from heated MFA–

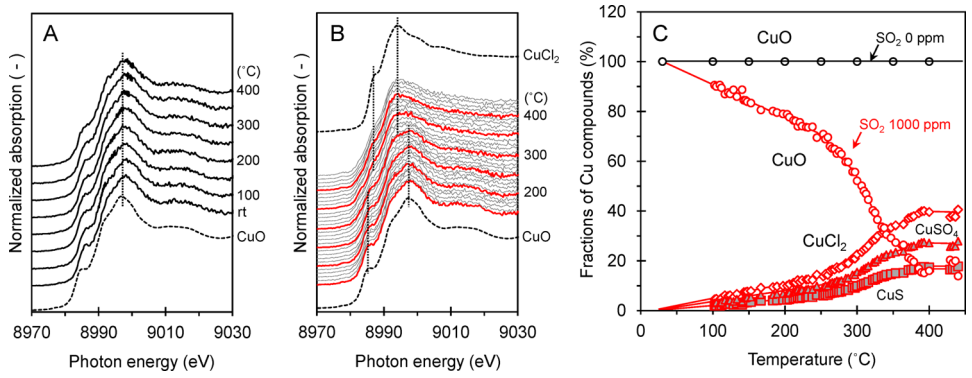

Figure 2. Copper (Cu) chemical forms as a function of temperature in model fly ash containing cupric oxide (CuO). (A) In situ Cu K-edge XANES spectra under no SO_2 gas stream. (B) In situ Cu K-edge XANES spectra under a 1000 ppm of SO_2 gas stream. (C) Fractions of Cu compounds by linear combination fitting of XANES under a (black) 0 and (red) 1000 ppm of SO_2 gas stream.

CuO and −$CuCl_2$ increased and decreased, respectively, with increased SO_2 injection. ∑CBzs, ∑PCBs, ∑PCDDs, and ∑PCDFs in MFA−CuO under 500−1000 ppm of SO_2 gas streams showed 12−27 (A1 in Figure 1), 13−32 (B1), 310−1100 (C1), and 20−38 (D1) times higher concentrations, respectively, than levels under a no-SO_2 gas stream. WHO-TEQ concentrations of ∑DL-PCBs, ∑PCDDs, and ∑PCDFs showed the same increasing trends (Figure S3, Supporting Information). So, toxicity of PCDD/Fs and PCBs was also increased in MFA−CuO by SO_2 gas injection. As a result of the marked increases in PCDD formation with SO_2 gas, PCDD/PCDF ratios under 500 and 1000 ppm of SO_2 gas streams had higher values (5.7 and 11, respectively) than that under no SO_2 gas (0.38). Selective formation of specific PCDD congeners, such as 1,3,6,8- and 1,3,7,9-T4CDD and 1,2,3,6,7,8- and 1,2,3,7,8,9-H6CDD, represented 4.7, 6.9, and 7.4% (residual ash) and 8.0, 24, and 29% (gas phase) of all congeners under the 0, 500, and 1000 ppm of SO_2 gas streams, respectively. These congeners have been reported to be the result of condensation reactions of precursors.[31] The ratio of PCDDs in MFA−CuO generated via condensation reactions may be increased, especially in the gas phase, by SO_2 gas injection.

∑CBzs, ∑PCBs, ∑PCDDs, and ∑PCDFs in MFA−$CuCl_2$ under 500−1000 ppm of SO_2 gas streams showed 48−65 (A1 in Figure 1), 52−66 (B1), 31−37 (C1), and 50−70% (D1) lower concentrations than that under a no-SO_2 gas stream. Similar moderate inhibition by SO_2 gas was reported in relation to PCDD/Fs using a model mixture (Mg−Al-silicate, KCl, $CuCl_2{\cdot}2H_2O$, and C) by Stieglitz et al.,[18] and PCBs and PCDD/Fs using an MSWI fly ash with added NaCl, $CuCl_2{\cdot}2H_2O$, and C by Pekárek et al.[32] WHO-TEQ concentrations of ∑PCDFs showed similar decreasing trend, although ∑DL-PCBs and ∑PCDDs hardly changed their WHO-TEQ concentrations by SO_2 injection (Figure S3, Supporting Information). It indicated that SO_2 gas had a weak influence to decrease toxic congeners of DL-PCBs and PCDDs in case of MFA−$CuCl_2$ system. PCDD/PCDF ratios increased slightly from 0.83 (no SO_2) to 1.2 and 1.8 (500 and 1000 ppm of SO_2, respectively). Specific PCDD congeners via condensation reactions described above represented 0.40, 2.0, and 5.2% (residual ash) and 12, 18, and 23% (gas phase) of all congeners under the 0, 500, and 1000 SO_2 gas streams, respectively. The ratios of PCDDs in MFA−$CuCl_2$ generated via condensation reactions may be increased, especially in the gas phase, by SO_2 gas injection, although de novo synthesis from carbon matrix might also occur.

Correlations among aromatic-Cls were calculated by using all data set of MFA−CuO and −$CuCl_2$ (n = 6). We found significant correlation between CBzs and PCDFs in ash phase (r = 0.974, p < 0.01) as shown in Table S4 (Supporting Information). In addition, significant correlations were also between PCDDs and PCDFs in gas phase (r = 0.991, p < 0.01) and between PCBs and PCDDs in ash phase (r = 0.834, p < 0.05). These relationships suggested similar behaviors by SO_2 injection. Moreover, CBzs might play a role as precursor of PCDFs in this heating system with SO_2 gas injection.

Thermochemical Behavior of CuO + KCl System. The *promoting* effect of SO_2 gas on MFA−CuO indicated that the thermochemical interaction among Cu (from CuO), Cl (from KCl), S (from SO_2 gas), and C (from AC) atoms occurred and contributed to increased aromatic-Cl formation. Thus, we discuss the distribution patterns of aromatic-Cls and attempted to identify changes in the chemical forms of Cu and S to clarify this promoting mechanism by SO_2 gas.

The distribution patterns of aromatic-Cls were affected by SO_2 gas. CBzs, PCBs, and PCDFs in residual ash of MFA−CuO increased in terms of highly chlorinated homologues, such as H6-benzene (A2 in Figure 1), H7- and O8-biphenyls (B2), and O8-CDF (D2), respectively, with increasing SO_2 gas injected. $CuCl_2$ promoted the formation of these highly chlorinated congeners (MFA−$CuCl_2$, 0 ppm of SO_2), consistent with a previous report using a similar MFA.[23] Additionally, MFAs including CuS with KCl, AC, and SiO_2 also showed similar highly chlorinated distribution patterns.[33] Because SO_2 gas was consumed by solid-phase copper (and potassium discussed below, ref reactions R3 and R4), the depletion of Cl_2 described in reaction R1 might not happen. There is a possibility that Cl_2 gas increased and then highly chlorinated congeners dominated. However, PCDDs in the residual ash of MFA−CuO showed increased middle-chlorinated homologues (H5- and H6-CDD) with SO_2 gas injection (C2 in Figure 1). The characteristic changes in the distribution pattern of PCDDs differed from that of other aromatic-Cls. In the gas phase, we could not analyze the distribution patterns of PCBs because almost no PCBs were detected with the GC/MS measurement system (B3 in Figure 1). CBzs in the gas phase showed increased T3-, T4-, and P5-benzenes under 1000 ppm of SO_2 gas (A3 in Figure 1). The distributions of PCDDs and PCDFs in the gas phase showed lower chlorinated patterns with higher concentrations of SO_2 gas (C3 and D3, respectively, in Figure 1).

Through in situ Cu K-edge XANES analysis, CuO did not change its chemical form during heating under the no-SO_2 gas stream. The XANES spectrum of the Cu K-edge maintained the same shape as the CuO reference spectrum during heating from room temperature to near 450 °C (Figure 2A). The LCF result also showed 100% CuO as the chemical form of Cu during heating (black line and symbols in Figure 2C). In contrast, we found that the XANES spectrum of the Cu K-edge changed markedly with increasing temperature under a 1000 ppm of $SO_2/O_2/N_2$ gas stream (Figure 2B). Although the characteristic shape of CuO (white line at 8997.5 eV, shoulder at 8985.5 eV) dominated at 300 °C, the spectrum shape changed to a lower white line (8994.5 eV) and a higher shoulder (8986.5 eV), close to the $CuCl_2$ reference spectrum. According to the LCF results, CuO in the model system decreased from 100 to 14%, and $CuCl_2$ increased from 0 to 41% (red lines and symbols in Figure 2C). In particular, large changes in the fractions of CuO and $CuCl_2$ were found between 250 and 400 °C. Minor fractions of Cu were identified as cupric sulfide (CuS, 0−18%) and sulfate ($CuSO_4$, 0−28%). Indeed, evidence of four Cu chemical forms (52% CuO, 23% $CuCl_2$, 9.9% CuS, 16% $CuSO_4$) was detected at 300 °C under the 1000 ppm of $SO_2/O_2/N_2$ gas stream (Figure 2C).

The interaction of gas-phase S with SO_2 gas and solid-phase chemicals was clarified using the S K-edge NEXAFS technique. CuO mounted on carbon tape showed a tiny peak at 2479 eV (Figure 3b), likely due to slight contamination of S in the carbon tape (Figure 3a). After heating MFA−CuO at 300 °C under a 1000 ppm of $SO_2/O_2/N_2$ gas stream, a specific spectrum of the S K-edge was measured (Figure 3d). The white line at 2480 eV had a strong intensity and a different energy from the contaminating S in the carbon tape. The energy position of the white line was the same as the K_2SO_4 and $CuSO_4{\cdot}5H_2O$ reference spectra, and the postedge feature was close to K_2SO_4 (Figure 3g,h). The LCF results indicated that the S consisted of 61% K_2SO_4 and 39% $CuSO_4{\cdot}5H_2O$ (Figure 3). Gas-phase S interacted thermally with solid-phase Cu and K, and then both K_2SO_4 and $CuSO_4{\cdot}5H_2O$ were generated in the solid phase. The KCl + AC (5N) MFA showed no change after heating at 300 °C under a 1000 ppm of $SO_2/O_2/N_2$ gas stream (Figure 3c). Thus, only the CuO + KCl + AC (5N) system interacted with the SO_2 gas.

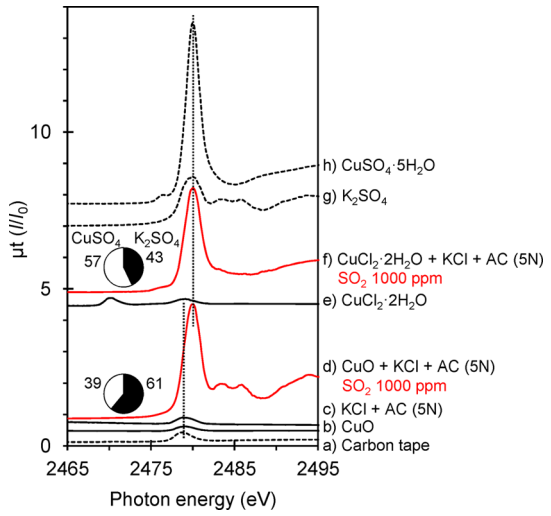

Figure 3. Raw sulfur K-edge NEXAFS spectra of (a) carbon tape; (b) cupric oxide (CuO); (c and d) model fly ash (MFA) containing KCl + AC (5N) and CuO + KCl + AC (5N) after heating at 300 °C for 30 min under a 1000 ppm of SO_2 gas stream; (e) cupric chloride dihydrate ($CuCl_2{\cdot}2H_2O$); (f) MFA containing $CuCl_2{\cdot}2H_2O$ + KCl + AC (5N) after heating at 300 °C for 30 min under a 1000 ppm of SO_2 gas stream; (g) potassium sulfate (K_2SO_4); (h) cupric sulfate ($CuSO_4{\cdot}5H_2O$). (Insets) Circle graphs are linear combination fitting results of standardized spectra of (bottom) d and (top) f.

From these results, we suggest the following thermochemical reaction:

$$CuO(s) + 2KCl(s) + 2SO_2(g) + \frac{3}{2}O_2(g) \rightarrow K_2SO_4(s) + CuSO_4(s) + Cl_2(g) \quad (R3)$$

According to the change in Gibbs free energy ($\Delta G < 0$) based on thermodynamics calculations, this reaction R3 progresses spontaneously below 910 °C. Because the NEXAFS spectrum generally reflects near atoms, $CuSO_4{\cdot}5H_2O$ was similar to $CuSO_4$ in structure. Additionally, $CuCl_2$ was identified as the major fraction of Cu compounds at 300 °C under the 1000 ppm of $SO_2/O_2/N_2$ gas stream by in situ Cu K-edge XANES analysis. Thus, we also suggest the following reaction:

$$2CuO(s) + 2KCl(s) + 2SO_2(g) + O_2(g) \rightarrow K_2SO_4(s) + CuSO_4(s) + CuCl_2(s) \quad (R4)$$

Reaction R4 progresses spontaneously below 850 °C ($\Delta G < 0$). In a previous study, we reported catalytic and direct chlorination of a C matrix by $CuCl_2$.[24,27] The C matrix was chlorinated in the case of MFA−CuO in the presence of SO_2 gas because reactions R3 and R4 progressed. "Real" MSWI fly ash contained trace Cu, and some part of the Cu exists as the oxide.[22,24,25] The major fraction of Cl in real MSWI fly ash was bonded with K (i.e., KCl).[19,20] Thus, reactions R3 and R4 may occur practically in real incinerators. Increasing PCDD/Fs with injected SO_2 gas into MFAs has been reported previously,[13,18] which was likely at least partly caused by this mechanism, related to the interaction between SO_2 gas and the solid-phase CuO + KCl system.

Thermochemical Behavior of $CuCl_2$ + KCl System. In contrast, aromatic-Cl generation with MFA−$CuCl_2$ was inhibited by SO_2 gas. To understand the inhibitory mechanism(s) of SO_2 gas, we also analyzed the distribution patterns of aromatic-Cls and the Cu and S K-edge X-ray absorption spectroscopic results.

Homologue distributions of CBzs, PCBs, and PCDFs in residual ash from MFA−$CuCl_2$ did not change their patterns under an SO_2 gas stream (A2, B2, and D2 in Figure 1, respectively). Under a no-SO_2 gas stream, formation of these aromatic-Cls was catalyzed by $CuCl_2$. These findings indicated that thermochemical formation paths of such aromatic-Cls were apparently not influenced by SO_2 gas and $CuCl_2$ played the role of a main catalyst. Because the total amounts of CBzs, PCBs, and PCDFs were reduced by SO_2 gas injection, the ratio of $CuCl_2$ in terms of Cu chemical form might have been decreased by the SO_2 gas. As a result of LCF analysis of in situ Cu K-edge XANES at 300 °C, the fraction of $CuCl_2$ under the 1000 ppm of SO_2 gas stream did show a lower value (53%) than with no SO_2 gas (64%; Figure 4C). PCDDs in the residual ash showed specific changes to a low-chlorinated distribution pattern (especially, T4-, H5-, and H6-CDDs) with SO_2 gas injection (C2 in Figure 1). This trend was also found in CBzs, PCDDs,

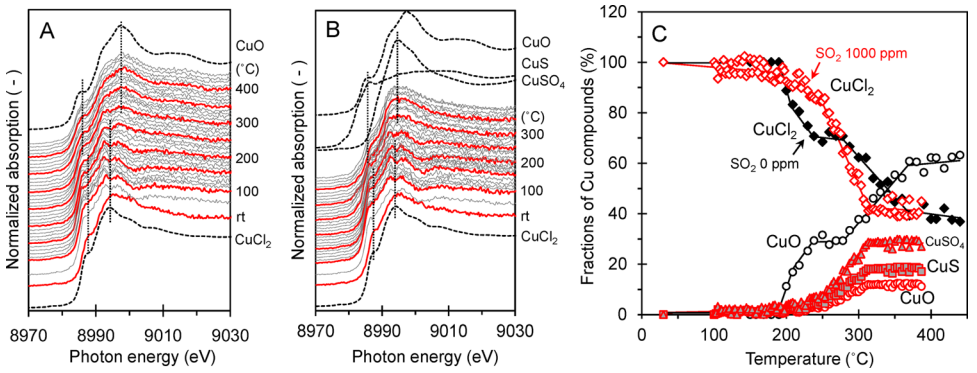

Figure 4. Copper (Cu) chemical forms as a function of temperature in the case of model fly ash containing cupric chloride dehydrate ($CuCl_2 \cdot 2H_2O$). (A) In situ Cu K-edge XANES spectra under a no-SO_2 gas stream. (B) In situ Cu K-edge XANES spectra under a 1000 ppm of SO_2 gas stream. (C) Fractions of Cu compounds by linear combination fitting of XANES spectra under (black) 0 and (red) 1000 ppm of SO_2 gas stream.

and PCDFs in the gas phase (A3, C3, and D3, respectively, in Figure 1). These changes in the distribution patterns of aromatic-Cls indicated thermochemical changes in the Cu by the SO_2 gas.

Cu K-edge XANES spectrum changed with temperature under the O_2/N_2 gas stream (Figure 4A), consistent with our previous report of similar in situ Cu K-edge XANES measurements.[27] The $CuCl_2$ form decreased from 100 to 40%, and the oxide form increased from 0 to 60% during heating from 200 to 400 °C (black lines and symbols in Figure 4C). Thus, the thermochemical change in $CuCl_2$ influenced oxidative breakdown of carbon matrix,[27,31] chlorinated the C matrix directly,[27] and catalyzed the formation of aromatic-Cls,[24] which related to de novo synthesis. With 1000 ppm of SO_2 in the gas stream, the Cu K-edge XANES spectrum had a different shape from that with no SO_2 gas. Above 300 °C, the spectrum shape was similar, and a white line at 8994.5 eV ($CuSO_4$) and the same pre-edge at 8985.5 eV (CuS and CuO) were evident (Figure 4B). $CuSO_4$ and CuS increased their fractions in Cu chemical form from 200 to 310 °C and maintained their fractions above that (30% and 19%, respectively, subtotal 49%) by LCF analysis (red lines and symbols in Figure 4C). Thus, the main part of the Cu was bonded with S through a thermochemical interaction between the SO_2 gas and the MFA−$CuCl_2$ system.

Before heating, negligible contamination of S was observed in $CuCl_2 \cdot 2H_2O$ (Figure 3e). S in the SO_2 gas interacted with solid-phase Cu and K, and then 57% $CuSO_4 \cdot 5H_2O$ and 43% K_2SO_4 were the chemical forms of S in the solid phase after heating to 300 °C, as analyzed by S K-edge NEXAFS (Figure 3f).

Compared with O_2/N_2 gas, 1000 ppm of $SO_2/O_2/N_2$ gas showed a lower fraction of CuO above 200 °C (Figure 4c). Thus, CuO may change mainly to $CuSO_4$ and CuS. According to the S K-edge NEXAFS results, K_2SO_4 was also generated in the solid phase (Figure 3f). Thus, reactions R3 and R4 would seem to progress to some degree. Additionally, the fraction of $CuCl_2$ with SO_2 gas injection was lower than that with no SO_2 gas from 280 to 350 °C (Figure 4C). The fraction of $CuSO_4$ in MFA−$CuCl_2$ (57%) was larger than that in MFA−CuO (39%) after heating at 300 °C (Figure 3). This result indicated the presence of pathways other than reactions R3 and R4. Indeed, from the analytical results, some $CuCl_2$ was converted to $CuSO_4$ by SO_2 gas, according to the following reaction:

$$CuCl_2(s) + SO_2(g) + O_2(g) \rightarrow CuSO_4(s) + Cl_2(g) \quad \text{(R5)}$$

This reaction progressed spontaneously below 910 °C ($\Delta G < 0$). Congener distributions and these reaction paths suggested that the inhibitory effect on aromatic-Cls in MFA−$CuCl_2$ by SO_2 gas was caused by partial sulfation of $CuCl_2$ via reaction R5.

Influence of Cu Chemical Form on the Role of SO_2. In the present study, we focused on gas−solid reactions. As a result, the solid-phase inorganic Cl (the KCl in this study) played an important role as a "Cl source" to form Cl gas and solid-phase $CuCl_2$ through reactions R3 and R4, respectively. However, these reactions did not progress without CuO in solid phase, as supported by the lack of change in S K-edge NEXAFS using the KCl + AC (5N) system (Figure 3c). A thermochemical interaction among SO_2 gas and the coexisting solid-phase CuO and KCl triggered the formation of relatively highly chlorinated aromatic-Cls, such as PCDFs, PCBs, and CBzs, but not PCDDs.

In contrast, $CuCl_2$ was suppressed in its promoting effect in generating aromatic-Cls by SO_2 gas injection. Although $CuCl_2$ was oxidized thermally under both SO_2 and no-SO_2 conditions (Figure 4c), partial sulfation of $CuCl_2$ occurred in the presence of SO_2 gas via reaction R5. This sulfation contributed to decreasing the fraction of $CuCl_2$ during the thermochemical formation of aromatic-Cls (280−350 °C). Most congener distribution patterns of aromatic-Cls in the solid phase did not change, except for PCDDs (A2, B2, and D2 in Figure 1). Thus, the decreased $CuCl_2$ fraction was a major factor in inhibiting aromatic-Cls formation.

We found odd behaviors of PCDDs with SO_2 gas injection. In the solid phase, congener distribution patterns of PCDDs showed low-chlorinated patterns in both MFA−CuO and −$CuCl_2$ (C2 in Figure 1). Although ∑PCDDs increased unexpectedly in MFA−CuO with SO_2 gas injection, a slight decrease in ∑PCDDs was found in MFA−$CuCl_2$ (C1 in Figure 1). Because CuO was generated in the MFA−$CuCl_2$ system and changed its chemical form to $CuSO_4$ (major) and CuS (minor; Figure 4C), reactions R3 and R4 also progressed. Thus, the low-chlorinated pattern and slight decrease in PCDDs could be explained. MFA−$CuCl_2$ showed partially the same formation paths to generate aromatic-Cls as the MFA−CuO system under an SO_2 gas stream.

CuS was identified as a minor part of the Cu chemical forms by in situ Cu K-edge XANES analyses of MFA−CuO and

dx.doi.org/10.1021/es503679c | Environ. Sci. Technol. 2014, 48, 13644−13651

$-CuCl_2$ under an SO_2 gas stream (Figures 2C and 4C, respectively). However, S K-edge NEXAFS did not detect CuS after heating at 300 °C under the SO_2 gas stream (Figure 3) because the amount of CuS was lower compared to $CuSO_4$, and almost all S was present as $CuSO_4$ and K_2SO_4. In our previous study, we reported that a CuS + KCl system promoted the thermochemical formation of highly chlorinated aromatic-Cls.[33] Thus, the minor amount of CuS also contributed to generating some aromatic-Cls with SO_2 gas injection.

From our results, the contrasting effects of SO_2 gas were strongly dependent on the oxide/chloride ratio of Cu in the fly ash. In "real" MSWI fly ash, Cu exists as the oxide and chloride.[20,22,23] A high S/Cl ratio resulted in no inhibition of PCDD/Fs with coal cofiring in MFA.[17] In this case, we suggest one possible reason is the low fraction of $CuCl_2$ in the MFA. The oxide/chloride ratio of Cu was not affected by the S/Cl ratio because most of the Cl was in the form of inorganic chlorides.[19,20] The chemical form of Cu (especially the oxide/chloride ratio) was thought to be a critical factor in controlling the formation of aromatic-Cls using SO_2 gas. In addition, our mechanism-based study helps to explain previous seemingly contradictory results when using SO_2 gas and similar experiments.

■ ASSOCIATED CONTENT

Supporting Information

Supporting Information includes QA/QC of GC/MS measurement, concentrations of chlorinated aromatics in MFA containing cupric oxide (Table S1) and chloride (Table S2), ash/gas ratios of chlorinated aromatics in MFAs (Table S3), Pearson's correlation coefficients among chlorinated aromatics (Table S4), a photo of in situ T-type cell and temperature profile during the in situ experiment (Figure S1), ash/gas ratios of CBzs, PCBs, PCDD/Fs (Figure S2), and WHO-TEQ concentrations of DL-PCBs and PCDD/Fs (Figure S3). This material is available free of charge via the Internet at http://pubs.acs.org.

■ AUTHOR INFORMATION

Corresponding Author

*E-mail: fujimori.takashi.3e@kyoto-u.ac.jp.

Notes

The authors declare no competing financial interest.

■ ACKNOWLEDGMENTS

We thank the staff and students of the Environmental Design Engineering Lab., Kyoto University, for help with XAFS measurements; K. Nitta, T. Ina, K. Kato, and T. Uruga (BL01B1) for support with in situ Cu K-edge XANES measurements at SPring-8 (Proposals 2010B1297, 2012B1192); Y. Kitajima (BL-11B) for help with S K-edge NEXAFS measurements at the Photon Factory (Proposal 2007G069 and 2012G021). T.F. acknowledges the financial support by a Grant-in-Aid for Young Scientists (A) from JSPS, Japan (No. 26701012). We also acknowledge the financial support by a Grand-in-Aid for Scientific Research (B) from JSPS, Japan (No. 25289171).

■ REFERENCES

(1) Huang, H.; Buekens, A. On the mechanisms of dioxin formation in combustion processes. *Chemosphere* **1995**, *31*, 4099−4117.

(2) Addink, R.; Olie, K. Mechanisms of formation and destruction of polychlorinated dibenzo-*p*-dioxins and dibenzofurans in heterogeneous systems. *Environ. Sci. Technol.* **1995**, *29*, 1425−1435.

(3) Tuppurainen, K.; Halonen, I.; Ruokojärvi, P.; Tarhanen, J.; Ruuskanen, J. Formation of PCDDs and PCDFs in municipal waste incineration and its inhibition mechanisms: A review. *Chemosphere* **1998**, *36*, 1493−1511.

(4) Stanmore, B. R. The formation of dioxins in combustion systems. *Combust. Flame* **2004**, *136*, 398−427.

(5) Altarawneh, M.; Dlugogorski, B. Z.; Kennedy, E. M.; Mackie, J. C. Mechanisms for formation, chlorination, dechlorination and destruction of polychlorinated dibenzo-*p*-dioxins and dibenzofurans (PCDD/Fs). *Prog. Energy Combust. Sci.* **2009**, *35*, 245−274.

(6) Kimble, B. J.; Gross, M. L. Tetrachlorodibenzo-*p*-dioxin quantitation in stack-collected coal fly ash. *Science* **1980**, *207*, 59−61.

(7) Lindbauer, R. L.; Wurst, F.; Prey, T. Combustion dioxin suppression in municipal solid waste incineration with sulfur additives. *Chemosphere* **1992**, *25*, 1409−1414.

(8) Gullett, B. K.; Dunn, J. E.; Raghunathan, K. Effect of cofiring coal on formation of polychlorinated dibenzo-*p*-dioxins and dibenzofurans during waste combustion. *Environ. Sci. Technol.* **2000**, *34*, 282−290.

(9) Olie, K.; Vermeulen, P. L.; Hutzinger, O. Chlorodibenzo-*p*-dioxins and chlorodibenzofurans are trace components of fly ash and flue gas of some municipal incinerators in The Netherlands. *Chemosphere* **1977**, *6*, 455−459.

(10) Griffin, R. D. A new theory of dioxin formation in municipal solid waste combustion. *Chemosphere* **1986**, *15*, 1987−1989.

(11) Ruokojärvi, P. H.; Halonen, I. A.; Tuppurainen, K. A.; Tarhanen, J.; Ruuskanen, J. Effect of gaseous inhibitors on PCDD/F formation. *Environ. Sci. Technol.* **1998**, *32*, 3099−3103.

(12) Ruokojärvi, P. H.; Asikainen, A. H.; Tuppurainen, K. A.; Ruuskanen, J. Chemical inhibition of PCDD/F formation in incineration processes. *Sci. Total Environ.* **2004**, *325*, 83−94.

(13) Ryan, S. P.; Li, X.-D.; Gullett, B. K.; Lee, C. W.; Clayton, M.; Touati, A. Experimental study on the effect of SO_2 on PCDD/F emissions: Determination of the importance of gas-phase versus solid-phase reactions in PCDD/F formation. *Environ. Sci. Technol.* **2006**, *40*, 7040−7047.

(14) Gullett, B. K.; Bruce, K. R.; Beach, L. O. Effect of sulfur dioxide on the formation mechanism of polychlorinated dibenzodioxin and dibenzofuran in municipal waste combustors. *Environ. Sci. Technol.* **1992**, *26*, 1938−1943.

(15) Gullett, B. K.; Bruce, K. R.; Beach, L. O.; Drago, A. M. Mechanistic steps in the production of PCDD and PCDF during waste combustion. *Chemosphere* **1992**, *25*, 1387−1392.

(16) Mahle, N. H.; Whiting, L. F. The formation of chlorodibenzo-*p*-dioxins by air oxidation and chlorination of bituminous coal. *Chemosphere* **1980**, *9*, 693−699.

(17) Raghunathan, K.; Gullett, B. K. Role of sulfur in reducing PCDD and PCDF formation. *Environ. Sci. Technol.* **1996**, *30*, 1827−1834.

(18) Stieglitz, L.; Vogg, H.; Zwick, G.; Beck, J.; Bautz, H. On formation conditions of organohalogen compounds from particulate carbon of fly ash. *Chemosphere* **1991**, *23*, 1255−1264.

(19) Zhu, F.; Takaoka, M.; Shiota, K.; Oshita, K.; Kitajima, Y. Chloride chemical form in various types of fly ash. *Environ. Sci. Technol.* **2008**, *42*, 3932−3937.

(20) Fujimori, T.; Tanino, Y.; Takaoka, M.; Morisawa, S. Chlorination mechanism of carbon during dioxin formation using Cl-K near-edge X-ray-absorption fine structure. *Anal. Sci.* **2010**, *26*, 1119−1125.

(21) Addink, R.; Espourteille, F.; Altwicker, E. R. Role of inorganic chlorine in the formation of polychlorinated dibenzo-*p*-dioxins/dibenzofurans from residual carbon on incinerator fly ash. *Environ. Sci. Technol.* **1998**, *32*, 3356−3359.

(22) Fujimori, T.; Tanino, Y.; Takaoka, M. Coexistence of Cu, Fe, Pb, and Zn oxides and chlorides as a determinant of chlorinated aromatics generation in municipal solid waste incinerator fly ash. *Environ. Sci. Technol.* **2014**, *48*, 85−92.

(23) Fujimori, T.; Takaoka, M.; Takeda, N. Influence of Cu, Fe, Pb and Zn chlorides and oxides on formation of chlorinated aromatic compounds in MSWI fly ash. *Environ. Sci. Technol.* **2009**, *43*, 8053−8059.
(24) Takaoka, M.; Shiono, A.; Nishimura, K.; Yamamoto, T.; Uruga, T.; Takeda, N.; Tanaka, T.; Oshita, K.; Matsumoto, T.; Harada, H. Dynamic change of copper in fly ash during de novo synthesis of dioxins. *Environ. Sci. Technol.* **2005**, *39*, 5878−5884.
(25) Takaoka, M.; Shiono, A.; Yamamoto, T.; Uruga, T.; Takeda, N.; Tanaka, T.; Oshita, K.; Matsumoto, T.; Harada, H. Relationship between dynamic change of copper and dioxin generation in various fly ash. *Chemosphere* **2008**, *73*, S78−S83.
(26) Takasuga, T.; Makino, T.; Tsubota, K.; Takeda, N. Formation of dioxins (PCDDs/PCDFs) by dioxin-free fly ash as a catalyst and relation with several chlorine-sources. *Chemosphere* **2000**, *40*, 1003−1007.
(27) Fujimori, T.; Takaoka, M. Direct chlorination of carbon by copper chloride in a thermal process. *Environ. Sci. Technol.* **2009**, *43*, 2241−2246.
(28) Fujimori, T.; Tanino, Y.; Takaoka, M.; Morisawa, S. Chlorination mechanism of carbon during dioxin formation using Cl-K near-edge X-ray-absorption fine structure. *Anal. Sci.* **2010**, *26*, 1119−1125.
(29) Fujimori, T.; Takaoka, M.; Tsuruga, S.; Oshita, K.; Takeda, N. Real-time gas-phase analysis of mono- to tri-chlorobenzenes generated from heated MSWI fly ashes containing various metal compounds: Application of VUV-SPI-IT-TOFMS. *Environ. Sci. Technol.* **2010**, *44*, 5528−5533.
(30) Stieglitz, L.; Zwick, G.; Beck, J.; Bautz, H.; Roth, W. Carbonaceous particles in fly ash—A source for the de-novo-synthesis of organochlorocompounds. *Chemosphere* **1989**, *19*, 283−290.
(31) Luijk, R.; Akkerman, D. M.; Slot, P.; Olie, K.; Kapteijn, F. Mechanism of formation of polychlorinated dibenzo-*p*-dioxins and dibenzofurans in the catalyzed combustion of carbon. *Environ. Sci. Technol.* **1994**, *28*, 312−321.
(32) Pekárek, V.; Punčochář, M.; Bureš, M.; Grabic, R.; Fišerová, E. Effects of sulfur dioxide, hydrogen peroxide, and sulfuric acid on the de novo synthesis of PCDD/F and PCB under model laboratory conditions. *Chemosphere* **2007**, *66*, 1947−1954.
(33) Fujimori, T.; Takaoka, M. Thermochemical chlorination of carbon indirectly driven by an unexpected sulfide of copper with inorganic chloride. *J. Hazard. Mater.* **2011**, *197*, 345−351.